

*Chapter 6*DESIGN OF ROBUST ATTACHMENT OF BIPYRIDINE LIGANDS TO SI
FOR THE IMMOBILIZATION OF HOMOGENEOUS CATALYSTS.

With contributions from James D. Blakemore, Robert J. Nielsen, Bruce S. Brunschwig,
Nathan S. Lewis, Petter Persson and William A. Goddard III

Introduction

In previous chapters, we have focused on homogeneous (or solution phase) catalysts for the production of chemical fuels.^{1,2} In general, however, catalysts of interest can either be homogenous or heterogeneous (a different phase than the surroundings), each with their advantages. Heterogeneous systems^{3,4} offer the advantage of simplified product separation; however single product selectivity can be difficult to achieve, but is key to the efficiency and productivity of fuel-forming devices. Homogenous electrocatalysts are well-known for their selectivity and rate and have been quite successful at selective production of solar fuels; however, product and catalyst separation can be difficult and expensive.⁵⁻⁸ By immobilizing a homogeneous catalyst to the surface of an electrode, one can ideally combine the advantages of the two systems, while making homogeneous catalysts better for industrial use.⁹⁻¹³

Early work on surface immobilization of electrocatalysts often saw the catalysts polymerize on the surface.^{14,15} Non-covalent attachment through π - π stacking of a catalyst to an electrode has seen moderate success. Using a pyrene-appended (bpy)Re(CO)₃(Cl) [bpy = 2,2'-bipyridyl] catalyst on graphitic carbon electrodes, CO₂RR to CO was achieved. TON of 58 was reached with no H₂ produced, implying success at achieving single product selectivity. However, over the course of several hours, loss of activity was seen due to detachment of the catalyst from the electrode.¹⁶ Kang et al. saw success with their (POCOP)Ir catalyst, which was similarly pyrene-appended to a carbon nanotube gas diffusion electrode. They saw catalysis over 8 hours with a TON of over 54,000.¹⁷ While covalent attachment of an electrocatalyst to an electrode seems like it should be more robust, there has been difficulty in creating a working system.¹⁸ Some covalently-bound catalysts and complexes have displayed stability under reductive conditions, including Co porphyrine systems attached to conductive diamond,¹⁹ vinyl ferrocene on the (111)

surface of Si²⁰, Co terpyridine catalysts grafted onto glassy carbon surfaces,²¹ and Rh catalysts incorporated into graphite surfaces.²² In the Co-porphyrine system, a long sp³ alkane group with a terminal azide was coupled with an alkyne in a Cu^I-catalyzed click reaction (CuAAC) to covalently bind it to conductive diamond. The catalyst was stable for at least 1000 electrochemical cycles and showed a turnover frequency (TOF) of 0.8 s⁻¹ for reduction of CO₂ to CO¹⁹. In the vinyl ferrocene system, a chlorinated Si (111) surface reacted with vinyl-tagged ferrocene. The remaining surface sites were then terminated with methyl groups, using a methyl Grignard reagent. Stable electrochemical cycling was observed. However, it was unclear how the attachment reaction proceeded mechanistically. Despite analogous reactions suggesting that upon attachment, the chlorine would be bound to the linker, little Cl was detected by XPS. Additionally, no IR stretch from a C-C double bond is observed.²³

Recent work by Lattimer et al. reported attachment of UV-induced attachment of vinyl-tagged bpy transition metal catalyst moiety. The bpy can then undergo cyclometallation to form (bpy)Rh(Cp*)(Cl), (bpy)Ir(Cp*)(Cl), and (bpy)Re(acac)₂ [Cp* = pentamethylcyclopentadienyl, acac = acetylacetonate] surface immobilized catalysts. While experimental evidence showed attachment had been made, upon cyclic voltammetry measurements, the complexes decayed within ~3 electrochemical cycles.²⁰

In this work, we study the vinyl bipyridine linker system computationally to elucidate the failure mechanism and provide potential solutions to increase the robustness of this system. This presents an interesting challenge, both due to the multiscale nature of the project and the ubiquity of bpy ligands in catalysis.²⁴⁻²⁷ Previous computational work has investigated surface immobilized catalysis in photocatalytic systems²⁸, as well as studying immobilized electrocatalysts on Au clusters for comparison to spectroscopy.²⁹

Methods

All geometry optimizations are completed with the B3LYP functional^{30,31} with Los Alamos small core potential on transition metals.³² Double ζ basis sets were used on transition metals and 6-311G** basis set were used on organic atoms.^{33,34} Poisson Boltzmann polarizable continuum acetonitrile solvent was also used in geometry optimizations. In all spin density and orbital plots *iso* values of 0.005 were used. Silicon clusters were cut along the (111) plane initially using

Crystal³⁵, then trimmed on the sides to minimize number of doubly H terminated sides. A similar method has been previously employed for oxide clusters.^{36,37} The clusters were designed to be large enough to enable a full ring of Me-Si bonds around the primary bond, in order to minimize the bending of neighboring Me-Si units outward. This bending had been seen in smaller clusters and was shown to affect the electronic behavior of the clusters.³⁸ Energies for large clusters consist only of electronic and solvation components, due to their large size.

The mechanism for dissociation including transition state calculations was calculated on tristrimethylsilane molecules, as frequency calculations were computationally intractable on the large clusters. All tristrimethylsilane complexes are optimized as per the methods above, however full free energies were calculated involving single point electronic energies, entropies, and enthalpies, in accordance with previously used methods.^{39,40} The calculation for single point energies is as follows:

$$G = E_{M06} + G_{solv} + E_{ZPE} + H_{vib} + H_{TR} - T(S_{vib} + S_{elec})$$

Zero point energies, E_{ZPE} , vibrational enthalpies, H_{vib} , and vibrational and electronic entropies, S_{vib} and S_{elec} respectively, were taken from frequency calculations. Translational and rotational enthalpies were calculated as $^{12}/_2 k_B T$. Single point electronic energies were calculated with M06 functional⁴¹ and 6-311G**++ basis set.^{42,43} Transition states verified using frequency calculations and intrinsic reaction coordinate calculations. All calculations were completed in Jaguar.³⁸

Results and Discussion

Effect of Chlorination on the Linker

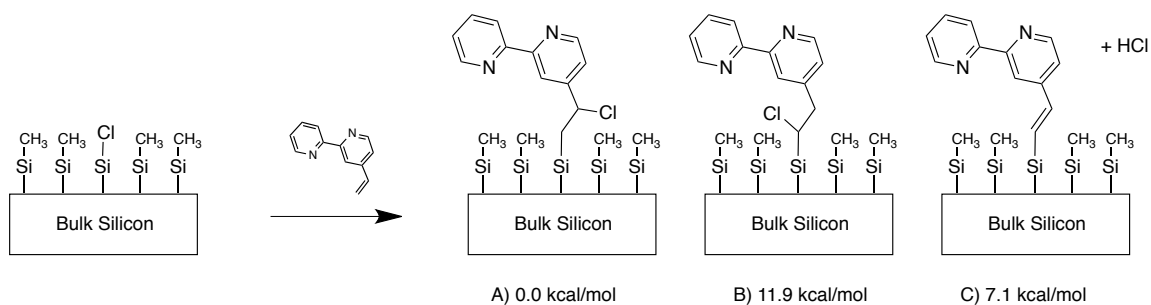


Figure 6.1: Relative energies (compared to A) of Cl binding motifs.

Previous experimental and computational work on the hydrogen terminated Si surface has proposed that photons excite electrons within the Si-H bond, breaking off a H radical and leaving a dangling Si radical.⁴⁴ This can then react with the vinyl-tagged molecules, which leaves a radical on the β -carbon of the vinyl linker. Recombination of the H and the vinyl radicals yield a linker in which the original H from the surface termination is located on the β -carbon of the linker.^{44,45} In the Cl-terminated surface, the analogous attachment scheme would yield a Cl on the β -carbon of the linker. Thermodynamic support for this mechanism can be seen in a comparison of free energies of cluster complexes with chlorine in different positions on the linker, as seen in Figure 6.1. In **A**, the Cl group has gone to the β -carbon. This is the lowest energy conformation. The energy of **B**, which features Cl on the α -carbon, is higher by 11.9 kcal/mol, largely due to unfavorable steric interaction with the neighboring methyl groups. This is further compared to the sp^2 analog of the linker **C**, which loses HCl in the process of linking, and is similarly higher in energy by 7.1 kcal/mol. This does not feature the same steric repulsion as **A**.

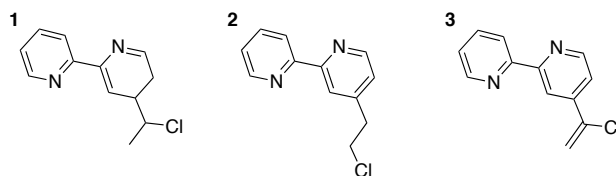


Figure 6.2: Molecular complexes with chlorinated linkers.

To further investigate the effect of chlorination on surface-bound complex, large basis set calculations were performed on the molecular bipyridine with Cl substituted throughout the linker, as shown in Figure 6.2. The molecular complexes were singly reduced as they would be on the surface under catalytic conditions. While reduced complexes **2** and **3** remained intact, reduced complex **1** decomposed into a chloride ion and a radical carbon linkage. The radical doublet was mostly centered on the β -carbon of the linker, as supported by atomic charges and spin populations, which are shown in Table 6.1. The spin density plot of the reduced complex is seen in Figure 6.3. It is of note that the spin density extends from one pyridine ring into the linker. The bpy ligand can be reversibly reduced in solution⁴⁶, so it should be able to host an electron without participation of the linker. However, this does not occur for the ligand with the Cl on the β carbon atom, complex **1**, and the linker degrades upon reduction.

Table 6.1: Atomic charges and spin populations of the reduced bpy complex

Atom	Atomic Charges	Spin
Cl	-0.88933	0.02026
β -carbon	-0.36476	0.69316
α -carbon	-0.10516	-0.05624

When the reduction process is repeated with the complex on a silicon cluster, the same decomposition occurs and the chlorine dissociates into solution. Examination of the spin density plot of the attached complex is similar to that of the molecular species, as shown in Figure 6.4.

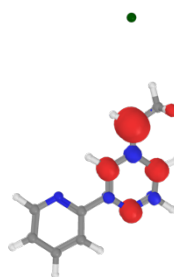


Figure 6.3: Spin density of the reduced chlorinated bpy complex. The chloride ion is released and settles at a distance 5.27 Å away from the β -carbon.

Together, the molecular and cluster calculations suggest the following decomposition pathway: during the attachment process, a chlorine radical formed by photoexcitation to break the Si-Cl bond recombines with a radical formed on the β -carbon to create a chlorinated linkage between the bpy complex and the Si surface (Figure 6.1, **A**). As this complex is reduced, the chlorine on the linker dissociates as a chloride ion, leaving a neutral doublet species on the β -carbon. This essentially reverses the attachment process, which allows the ν -bpy ligand to dissociate from the surface.

To test this hypothesis, we used tris(trimethyl)silane complex as the analogue for the silicon surface. The proposed mechanism can be seen in Scheme 6.1. Hydrogen terminated silanes have been previously shown to undergo the same photoactivation processes leading to the formation of a silyl radical and reaction with alkenes⁴⁷, so they are valuable analogues to our infinite process.

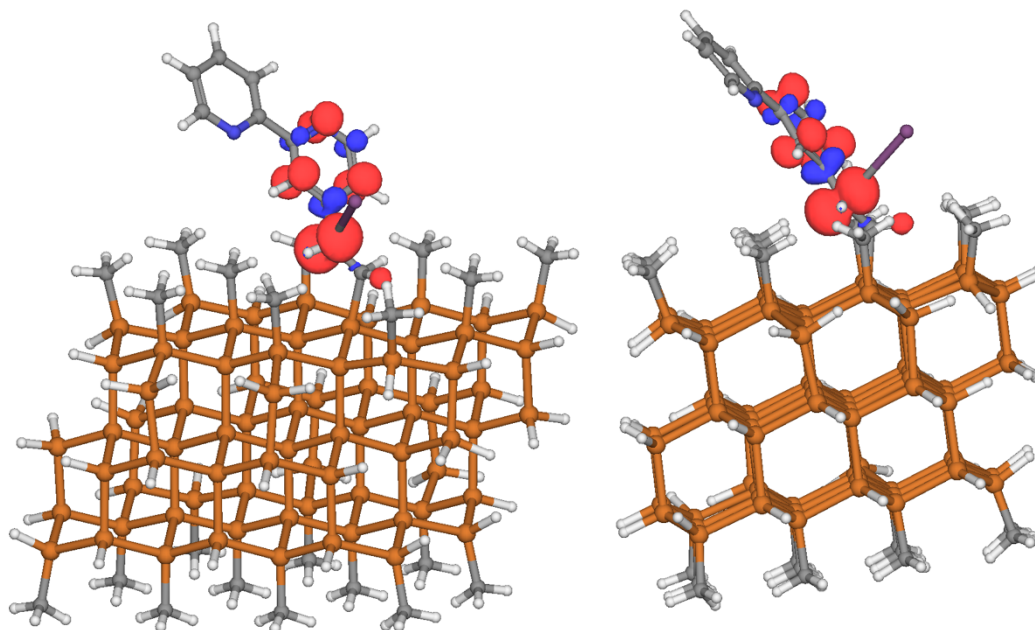
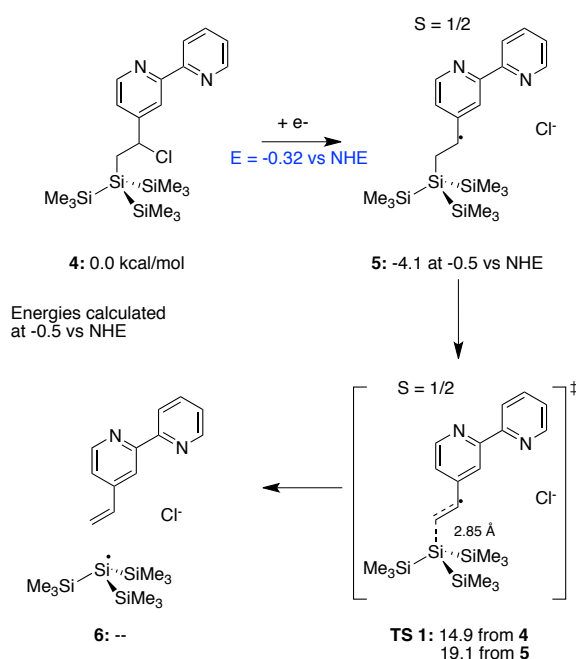


Figure 6.4: Spin density from two views on the reduced chlorinated complex **2** attached to a silicon cluster. The molecular and attached spin densities are quite similar to the molecular complex. The C-Cl distance is 3.62 Å, suggesting the chlorine has migrated from the linker.

The reduction of the chlorinated bpy system with loss of a chloride ion is calculated to occur at -0.32 V vs NHE, which can be verified experimentally. The overall barrier for the separation of the de-chlorinated bpy complex from the tris(trimethyl)silane is 14.9 kcal/mol, calculated with the free energy of an electron at -0.5 V vs NHE from the unreduced ground state, **4**. The barrier for dissociation from the immediately preceding step **5** is independent of the energy of the electron and the operating potential. This barrier is calculated to be 19.1 kcal/mol.



Scheme 6.1: The transition state for dissociation using a tristrimethylsilane toy system is shown in **TS 1**. While the overall barrier is dependent on the operating potential, the barrier energy from **5** is constant at 19.1 kcal/mol. This is accessible at room temperature. Additionally, the driving force for this complex gets stronger as more negative potentials are reached.

However, the overall barrier is dependent on the potential at which the reduction occurs. This dependence is shown in Figure 6.5. As the system is taken to more negative potentials, the loss of the bpy complex will occur even more quickly, such that once the system is at a potential of -1.1 V vs NHE, the barrier is nearly thermoneutral with the ground state. Additionally, bond strengths vary with the number of Si groups attached to the silane of interest⁴⁸, so in the practically infinite Si crystal, this dissociation may occur even more rapidly than predicted by the molecular calculation. Effectively, the chlorine on the linker weakens the attachment to the surface.

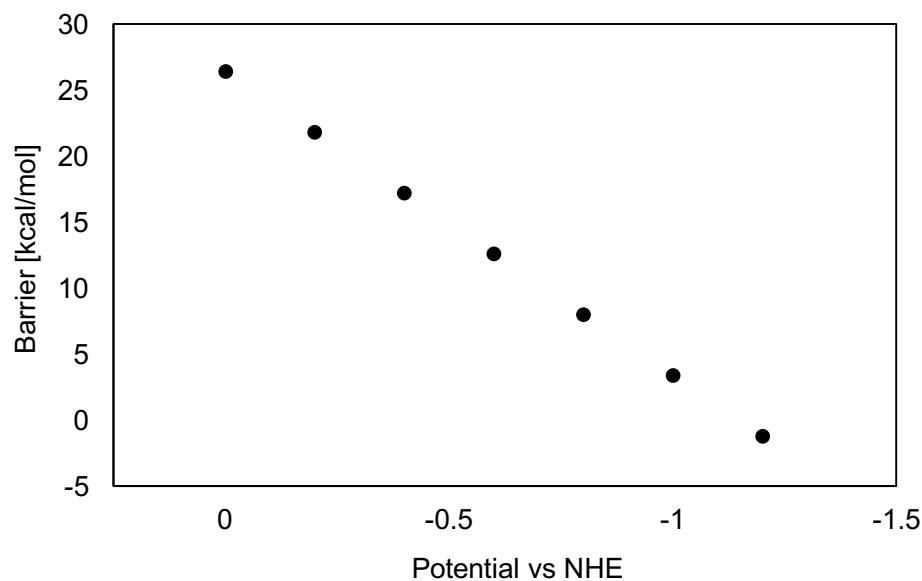


Figure 6.5: Overall dissociation barrier as a function of potential. As more negative potentials are reached, the dissociation becomes more kinetically favorable.

Other bpy systems as replacements

As analogous behavior can be seen between the molecular calculation and the cluster calculation, the molecular calculations can be used to screen complexes. One change that can be made is to use other halogens in the attachment process. Fluorine and bromine were attached to both the α - and β -carbons of the linker and the molecular complex was reduced in solution, as shown in Figure 6.6, complexes **7** and **8**.

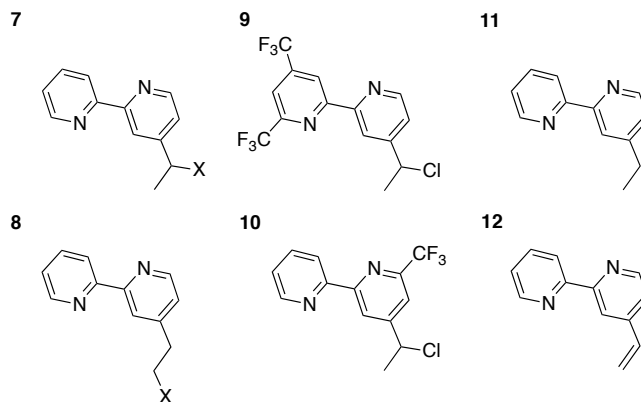


Figure 6.6: Molecular test analogues used to investigate ways to utilize bpy's non-innocent properties. In the halogenated species **7** and **8**, X = F, Br.

As bromine is typically classified as a better leaving group than chlorine, it is unsurprising that under reduction, the brominated ligand decayed in both positions. The fluorinated ligand, however, was stable under reduction in both positions, yielding an improvement upon the chlorinated ligand. Spin density plots for all modified complexes can be seen in Figure 6.7. The brominated case is quite similar to the chlorinated analogue, where the spin density extends into the linker. However, the fluorinated analogue shows much different behavior, with the bulk of the spin density isolated in the bpy, the expected non-innocent behavior. The fluorine does not appear to dissociate in the form of a fluoride ion.

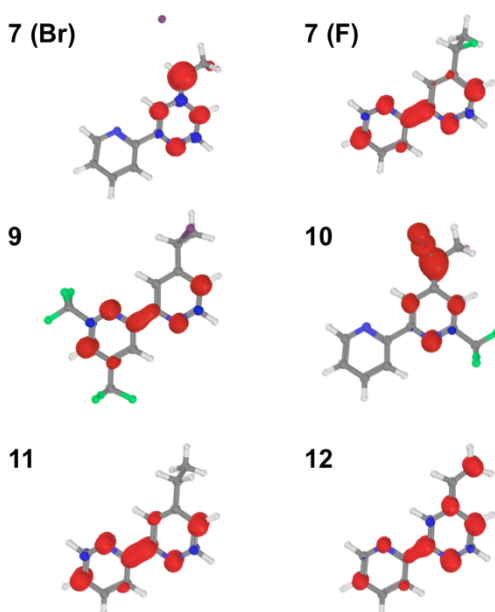


Figure 6.7: Spin density plots of the modified bpy ligands. In the fluorinated (**7F**), bis- CF_3 (**9**) and sp^3 -hybridized linker (**11**) cases, electron density is isolated on the bpy, behavior expected for the non-innocent ligand

From this behavior, it can be predicted that the fluorinated complex would be stable on the surface and would not degrade. The geometry and spin density plot of this complex is seen in Figure 6.8. In the reduced molecular complex, the C-F bond in the linker is 1.42 Å, whereas in the bound complex, the C-F bond is 1.44 Å. This is slightly lengthened; however, it could be due to the smaller basis set by which the cluster-molecule complexes are calculated. Similar to the molecular complex, the spin density is largely isolated on the bpy ligand, with only a small amount on the fluorine. The spin density on the surface-attached fluorine is 0.00645, while the

molecular species has a spin density of 0.00036 on the fluorine. While there is a difference, this is still insignificant to the amount on the C and N atoms of the bipyridal group, which ranges from 0.15 to 0.25 on both the molecular and surface-attached complexes. The difference in fluorine spin densities on the fluorine may be attributed to the difference in basis set used. What is more significant is that there is very little spin density on the β -carbon of the linker (0.01504).

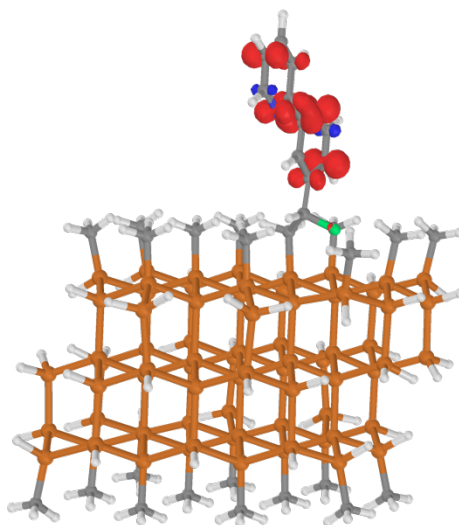


Figure 6.8: Spin density plot of the surface-attached fluorinated complex. Density is mostly confined to the bpy ligand.

It would appear that isolation of the added electron during reduction on the bpy ligand leaves the linker intact. Thus approaches to prevent the movement of electron density to the linker may be key to increasing the robustness of surface attached catalysts. One way of doing this is to add electron-withdrawing groups to the bpy to draw the electron off the linker. As hypothetical test cases, both 4'-(1-chloroethyl)-4,6-bis(trifluoromethyl)-2,2'-bipyridine (**9**) and 4-(1-chloroethyl)-6-(trifluoromethyl)-2,2'-bipyridine (**10**) were reduced and compared. Trifluoromethyl (CF_3) groups are both strongly electron-withdrawing⁴⁹ and meta-directing, so they were strategically placed to maximize electron density on the bpy moiety. The spin density plots of **9** and **10** are shown in Figure 6.6. While **9** shows improvement upon the original complex **2**, there is some residual spin density on the β -carbon of the linker. The C-Cl bond in the reduced complex **9** is 1.89 Å, whereas the unreduced complex **2** has a C-Cl bond of 1.87 Å, which suggests that though there is some spin density on the linker, it does not significantly

encourage dissociation of the chloride ion. Using one CF_3 group on the meta position to the vinyl linkage, as in complex **10**, does not appear to be an improvement upon the parent complex as the spin density again extends into the linker. The use of electron withdrawing groups on the bpy complex may prevent dissociation; however, their position is very important. To achieve this, asymmetric synthesis is necessary. Additionally, these groups may affect catalysis.

A potentially more successful approach would be to eliminate ionic groups on the linkers altogether, either through a sp^2 or sp^3 hybridized linker. These complexes, **11** and **12** respectively, and their spin densities can be seen in Figure 6.6. While both complexes do not degrade, it is important to note that the conjugation between the bpy and the vinyl linkage is quite clear, as spin density is delocalized over the entire complex. In the sp^3 ethyl linkage, the electron is fully confined to the bpy complex and none remains on the linker. Berry's work with Co porphyrin catalysts utilized a long (greater than 9 CH_2 units), largely sp^3 hybridized linkage that showed great stability.¹⁹ However, the linker is long enough that the catalyst could potentially fold over towards the surface, allowing for diffusional electron transport. Berry et al. reports that there was a change in the cyclic voltammogram of the system that showed settling after the first 300 cycles, suggesting that an ideal conformation may be found after some cycling.¹⁹ Electron hopping or tunneling through the linker would be unlikely with such a long linker. A short sp^3 hybridized linker would be ideal.

An acetylide sp hybridized linker was also explored, based on recent studies involving ethynyl and propynyl functionalization of Si^{50} and the modification of the Si band structure with fluorinated phenyl groups bound to the surface with these groups.⁵¹ In the past, sp hybridized groups have been used in dye-sensitized solar cells (DSSCs) in rigid rod constructions to make linkers that would not bend^{52,53}, and have been used in conjunction with bipyridine groups.⁵⁴ In order to investigate the possibility of using these groups as linkers, 4-ethynyl-2,2'-bipyridine moieties were reduced both molecularly and on the cluster, as is seen in Figure 6.9.

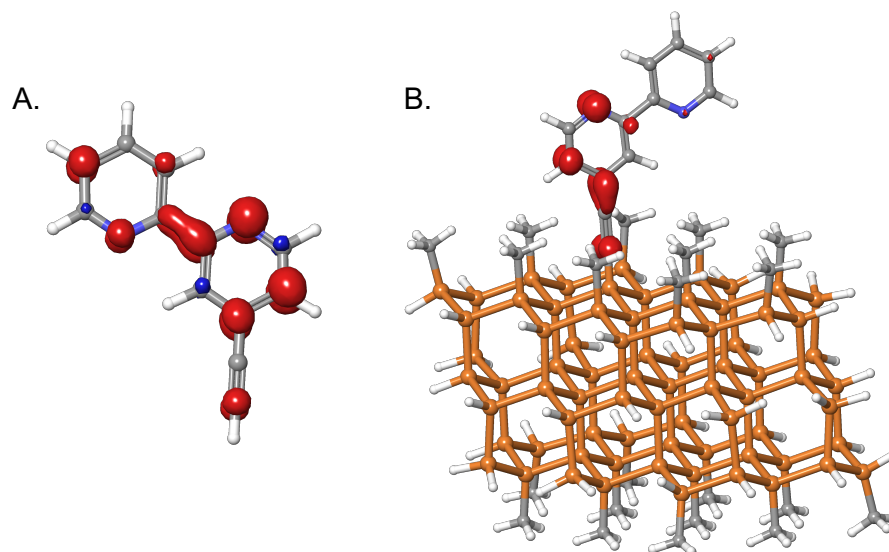


Figure 6.9: Spin density on reduced 4-ethynyl-2,2'-bipyridine A) in molecular form and B) on the cluster surface.

In Figure 6.9A, the spin density plot shows some spin density on the α -carbon, though none on the β -carbon. Once bound to the cluster (Figure 6.9B), we see that some electron density extends onto the β -carbon, but most of it is in the first pyridine ring and on the α -carbon, a departure from what has been previously seen. This is corroborated by the change in bond length upon reduction. In **2** bound to the cluster (see Figure 6.4), the C-C bond length in the linker changes from 1.54 Å to 1.48 Å, shortening due to the loss of the Cl. In contrast, in the sp hybridized system, the linker actually extends slightly, from 1.23 Å to 1.24 Å, much less change, however, than the chlorinated system. The triple bond here in this case may be helpful. By hosting some electron density, it may not be as stable as a fully sp^3 -hybridized case, but it appears to be more robust than the chlorinated linkers.

The rate of electron transfer through such a linker is critical. Using DSSCs as an analogue, Li et al. calculated that fully sp^3 hybridized linkers slowed electron injection from a dye into a TiO_2 cluster by a factor of ~ 7 relative to alkene linkers.⁵⁵ These times for electron injection are in the tens of femtoseconds range. However, even in seemingly fast or selective catalysts, the turnover frequencies are usually in $0.1\text{-}10\text{ s}^{-1}$.^{5,16,56} Often the rate-limiting step is not one that is electrochemical, but rather binding of the substrate, protonation, or hydride transfer. This means

that even with the slowed rate of electron transfer, the linker will not likely be the limit for the catalyst and all strategies should be pursued.

Conclusion

In this chapter, we have identified the thermodynamically preferred surface attachment structure in the attachment of vinyl bpy to a partially chlorinated Si(111) surface. This involves chlorination on the β -carbon of the linker, which inevitably leads to the electrochemical decomposition seen experimentally. In order to achieve this level of understanding, calculations were performed on Si clusters, as well as trimethyltrissilyl silane molecules. Future work involves expanding this analysis to periodic systems, though this is often difficult due to limitations in unit cell size and solvation. Several alternative systems for linking have been proposed, including replacing chlorine with fluorine, and using sp^3 and sp hybridized linkers. These options provide a blueprint for experimentally creating more robust surface attachments for electrochemical catalysts on Si.

References

- (1) Lewis, N. S.; Nocera, D. G. *Proc. Natl. Acad. Sci. USA* **2006**, *103*, 15729-15735.
- (2) Olah, G. A. *Angew. Chem. Int. Ed.* **2013**, *52*, 104-107.
- (3) Li, C. W.; Kanan, M. W. *J. Am. Chem. Soc.* **2012**, *134*, 7231-7234.
- (4) Kuhl, K. P.; Cave, E. R.; Abram, D. N.; Jaramillo, T. F. *Energy Environ. Sci.* **2012**, *5*, 7050-7059.
- (5) Kang, P.; Cheng, C.; Chen, Z.; Schauer, C. K.; Meyer, T. J.; Brookhart, M. J. *Am. Chem. Soc.* **2012**, *134*, 5500-5503.
- (6) Benson, E. E.; Kubiak, C. P.; Sathrum, A. J.; Smieja, J. M. *Chem. Soc. Rev.* **2009**, *38*, 89-99.
- (7) Costentin, C.; Robert, M.; Saveant, J.-M. *Chem. Soc. Rev.* **2013**, *42*, 2423-2436.
- (8) Jessop, P. G.; Joó, F.; Tai, C.-C. *Coord. Chem. Rev.* **2004**, *248*, 2425-2442.
- (9) Abruña, H. D. *Coord. Chem. Rev.* **1988**, *86*, 135-189.
- (10) Murray, R. W. *Acc. Chem. Rev.* **1980**, *13*, 135-141.
- (11) McCreery, R. L. *Chem. Rev.* **2008**, *108*, 2646-2687.
- (12) Wrighton, M. S. *Science* **1986**, *231*, 32-37.
- (13) Inglis, J. L.; MacLean, B. J.; Pryce, M. T.; Vos, J. G. *Coord. Chem. Rev.* **2012**, *256*, 2571-2600.
- (14) Chardon-Noblat, S.; Deronzier, A.; Ziessel, R.; Zsoldos, D. *J. Electroanal. Chem.* **1998**, *444*, 253-260.
- (15) Bolinger, C. M.; Story, N.; Sullivan, B. P.; Meyer, T. J. *Inorg. Chem.* **1988**, *27*, 4582-4587.
- (16) Blakemore, J. D.; Gupta, A.; Warren, J. J.; Brunschwig, B. S.; Gray, H. B. *J. Am. Chem. Soc.* **2013**, *135*, 18288-18291.
- (17) Kang, P.; Zhang, S.; Meyer, T. J.; Brookhart, M. *Angew. Chem.* **2014**, *126*, 8853-8857.
- (18) Sun, C.; Gobetto, R.; Nervi, C. *New J. Chem.* **2016**, *40*, 5656-5661.
- (19) Yao, S. A.; Ruther, R. E.; Zhang, L.; Franking, R. A.; Hamers, R. J.; Berry, J. F. *J. Am. Chem. Soc.* **2012**, *134*, 15632-15635.
- (20) Lattimer, J. R. C.; Blakemore, J. D.; Sattler, W.; Gul, S.; Chatterjee, R.; Yachandra, V. K.; Yano, J.; Brunschwig, B. S.; Lewis, N. S.; Gray, H. B. *J. Chem. Soc., Dalton Trans.* **2014**.
- (21) Elgrishi, N.; Griveau, S.; Chambers, M. B.; Bedioui, F.; Fontecave, M. *Chem. Comm.* **2015**, *51*, 2995-2998.
- (22) Oh, S.; Gallagher, J. R.; Miller, J. T.; Surendranath, Y. *J. Am. Chem. Soc.* **2016**, *138*, 1820-1823.
- (23) Lattimer, J. R. C.; Brunschwig, B. S.; Lewis, N. S.; Gray, H. B. *J. Phys. Chem. C* **2013**, *117*, 27012-27022.
- (24) Quintana, L. M. A.; Johnson, S. I.; Corona, S. L.; Villatoro, W.; Goddard, W. A.; Takase, M. K.; VanderVelde, D. G.; Winkler, J. R.; Gray, H. B.; Blakemore, J. D. *Proc. Natl. Acad. Sci. USA* **2016**, *113*, 6409-6414.
- (25) Bolinger, C. M.; Story, N.; Sullivan, B. P.; Meyer, T. J. *Inorg. Chem.* **1988**, *27*, 4582-4587.
- (26) Brennaman, M. K.; Dillon, R. J.; Alibabaei, L.; Gish, M. K.; Dares, C. J.; Ashford, D. L.; House, R. L.; Meyer, G. J.; Papanikolas, J. M.; Meyer, T. J. *J. Am. Chem. Soc.* **2016**, *138*, 13085-13102.
- (27) Blakemore, J. D.; Schley, N. D.; Balcells, D.; Hull, J. F.; Olack, G. W.; Incarvito, C. D.; Eisenstein, O.; Brudvig, G. W.; Crabtree, R. H. *J. Am. Chem. Soc.* **2010**, *132*, 16017-16029.
- (28) Durrell, A. C.; Li, G.; Koepf, M.; Young, K. J.; Negre, C. F. A.; Allen, L. J.; McNamara, W. R.; Song, H.-e.; Batista, V. S.; Crabtree, R. H.; Brudvig, G. W. *J. Catal.* **2014**, *310*, 37-44.
- (29) Clark, M. L.; Rudshteyn, B.; Ge, A.; Chabolla, S. A.; Machan, C. W.; Psciuk, B. T.; Song, J.; Canzi, G.; Lian, T.; Batista, V. S.; Kubiak, C. P. *J. Phys. Chem. C.* **2016**.
- (30) Becke, A. D. *J. Chem. Phys.* **1993**, *98*, 5648-5652.
- (31) Lee, C. T.; Yang, W. T.; Parr, R. G. *Phys. Rev. B* **1988**, *37*, 785-789.
- (32) Hay, P. J.; Wadt, W. R. *J. Chem. Phys.* **1985**, *82*, 299-310.
- (33) Francl, M. M.; Pietro, W. J.; Hehre, W. J.; Binkley, J. S.; Gordon, M. S.; Defrees, D. J.; Pople, J. A. *J. Chem. Phys.* **1982**, *77*, 3654-3665.
- (34) Hehre, W. J.; Ditchfie, R.; Pople, J. A. *J. Chem. Phys.* **1972**, *56*, 2257-2261.
- (35) Dovesi, R. O., R.; Civalleri, B.; Roetti, C.; Saunders, V. R.; Zicovich-Wilson, C. M. *Z. Kristallogr.* **2005**, *220*, 571-573.
- (36) Galynska, M.; Persson, P. In *Advances in Quantum Chemistry*; Sabin, J. R., Ed. 2014; Vol. 69, p 303-332.
- (37) Galynska, M.; Persson, P. *Int. J. Quantum Chem.* **2013**, *113*, 2611-2620.
- (38) Bochevarov, A. D.; Harder, E.; Hughes, T. F.; Greenwood, J. R.; Braden, D. A.; Philipp, D. M.; Rinaldo, D.; Halls, M. D.; Zhang, J.; Friesner, R. A. *Int. J. Quantum Chem.* **2013**, *113*, 2110-2142.
- (39) Johnson, S. I.; Nielsen, R. J.; Goddard, W. A. *ACS Catal.* **2016**, 6362-6371.

- (40) Zhou, M.; Johnson, S. I.; Gao, Y.; Emge, T. J.; Nielsen, R. J.; Goddard, W. A.; Goldman, A. S. *Organometallics* **2015**, *34*, 2879-2888.
- (41) Zhao, Y.; Truhlar, D. G. *Theor. Chem. Acc.* **2008**, *120*, 215-241.
- (42) Krishnan, R.; Binkley, J. S.; Seeger, R.; Pople, J. A. *J. Chem. Phys.* **1980**, *72*, 650-654.
- (43) Clark, T.; Chandrasekhar, J.; Spitznagel, G. W.; Schleyer, P. V. J. *Comp. Chem.* **1983**, *4*, 294-301.
- (44) Cicero, R. L.; Linford, M. R.; Chidsey, C. E. D. *Langmuir* **2000**, *16*, 5688-5695.
- (45) Buriak, J. M. *Chem. Mater.* **2014**, *26*, 763-772.
- (46) Saji, T.; Aoyagui, S. *J. Electroanal. Chem. Interfacial Electrochem.* **1975**, *58*, 401-410.
- (47) Chatgililoglu, C. *Chem. Rev.* **1995**, *95*, 1229-1251.
- (48) Wu, Y.-D.; Wong, C.-L. *J. Org. Chem.* **1995**, *60*, 821-828.
- (49) Hansch, C.; Leo, A.; Taft, R. W. *Chem. Rev.* **1991**, *91*, 165-195.
- (50) Plymale, N. T.; Kim, Y.-G.; Soriaga, M. P.; Brunschwig, B. S.; Lewis, N. S. *J. Phys. Chem. C* **2015**, *119*, 19847-19862.
- (51) Plymale, N. T.; Ramachandran, A. A.; Lim, A.; Brunschwig, B. S.; Lewis, N. S. *J. Phys. Chem. C* **2016**, *120*, 14157-14169.
- (52) Chitre, K.; Batarseh, A.; Kopecky, A.; Fan, H.; Tang, H.; Lalancette, R.; Bartynski, R. A.; Galoppini, E. *J. Phys. Chem. B* **2015**, *119*, 7522-7530.
- (53) Galoppini, E. *Coord. Chem. Rev.* **2004**, *248*, 1283-1297.
- (54) Wang, D.; Mendelsohn, R.; Galoppini, E.; Hoertz, P. G.; Carlisle, R. A.; Meyer, G. J. *J. Phys. Chem. B* **2004**, *108*, 16642-16653.
- (55) Li, J.; Wang, H.; Persson, P.; Thoss, M. *J. Chem. Phys.* **2012**, *137*.
- (56) Cosnier, S.; Deronzier, A.; Vlachopoulos, N. *J. Chem. Soc., Chem. Commun.* **1989**, 1259-1261.